Exploration of Rational Donor-Acceptor Adjustment Strategies to Achieve ACQ to AIE transformation and Their Potential Applications as Multi-functional AIEgens

Weiwei Zhang,[# a b] Yongbo Wei,[# a] Fen Lin,[# c] Yinyin Yao,[d] Xia Wang,[a] Yongxiao Sun,[a] Jingming Zhou,[a] Tong Wu,[a] Nannan Chen, [a]Yusheng Lu,[d]* Xiaoping Wu[b]* and Lijun Xie[a, b]*

[a] Fujian Provincial Key Laboratory of Screening for Novel Microbial Products, Fujian Institute of Microbiology, Fuzhou, Fujian 350007, PR China.

[b] College of Life Sciences, Fujian Agriculture and Forestry University, Fuzhou, Fujian 350002, PR China.

[c] Fujian Provincial Governmental Hospital, Fuzhou, Fujian Province 350000, PR China.

[d]Fujian-Taiwan-Hongkong-Macao Science and Technology Cooperation Base of Intelligent Pharmaceutics, College of Material and Chemical Engineering, Minjiang University, Fuzhou, Fujian 350108, China.

Supporting Information

1. Solvatochromic Properties

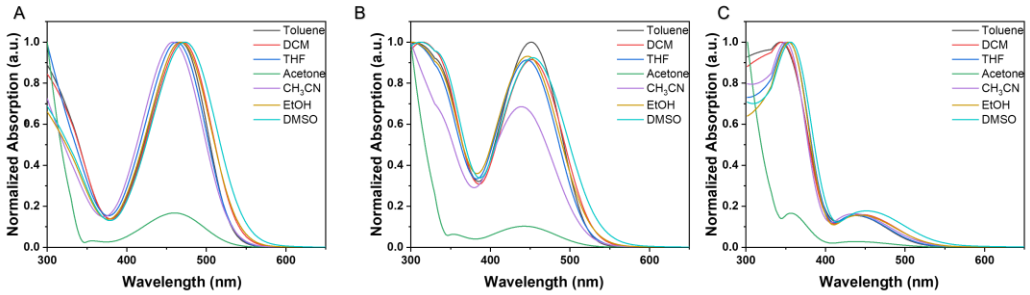

Figure S1. (A) Absorption spectra of **L1**, **L2** and **L3** in different solution (50 uM).

compound	Solvents	λ_{abs} (nm) [a]	λ_{em} (nm) [b]	Stokes shifts (nm) [c]	Δv (cm^{-1}) [d]
L1	DMSO	474	650	176	5712
	EtOH	468	628	160	5443
	CH_3CN	458	634	176	6061
	THF	462	616	154	5411
	DCM	470	610	140	4883
	Toluene	468	584	116	4244
L2	DMSO	454	694	240	7617
	EtOH	446	628	182	6497
	CH_3CN	440	674	234	7890
	THF	446	632	186	6598
	DCM	452	634	182	6351
	Toluene	450	594	144	5387
L3	DMSO	450	/	/	/
	EtOH	444	/	/	/
	CH_3CN	436	/	/	/
	THF	436	696	260	8567
	DCM	444	656	212	7278
	Toluene	438	600	162	6164

Table S1. The photo-physical data of **L1**, **L2** and **L3** in various solution with the concentration of 50 μM.

The solvatochromic Lippert-Mataga equation

$$\Delta v = \frac{2\Delta\mu^2}{hca^3}\Delta f + Const \quad (1)$$

$$\Delta f = \frac{\varepsilon - 1}{2\varepsilon + 1} - \frac{n^2 - 1}{2n^2 + 1} \quad (2)$$

Δv is the stokes shift, $\Delta \mu$ is the difference in the dipole moments in the ground and excited states, and h, c, and a stand for the Planck constant, the speed of light, and the Onsager solvent cavity radius, respectively. Δf is the orientation polarizability, ε is the dielectric constant and n is the refractive index.

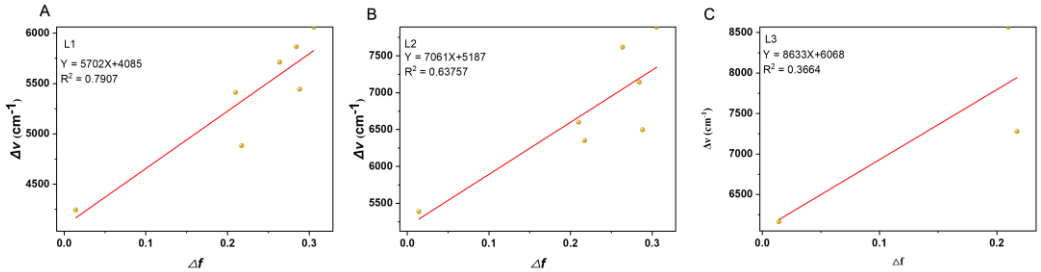

Figure S2. Beer-Lambert's plot and linear fitting of **L1** (A) and **L2** (B) and **L3** (C). (Y = 4085+5720X, R^2 = 0.7907; Y = 5187+7061X, R^2 = 0.63757; Y = 6068+8633X, R^2 = 0.3664)

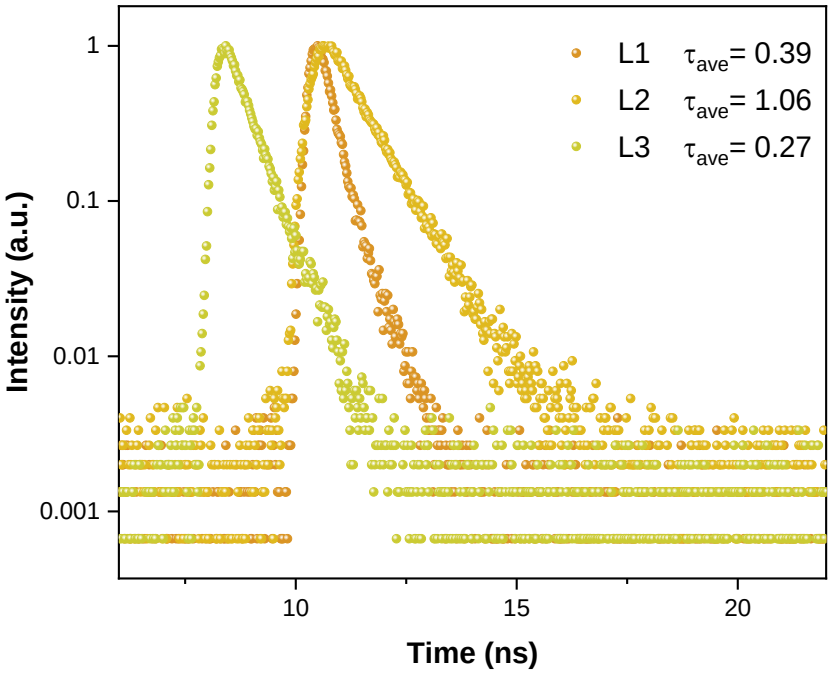

Figure S3. time-resolved photo luminescence of the samples about L1, L2 and L3 in toluene.

2. Aggregation-induced emission

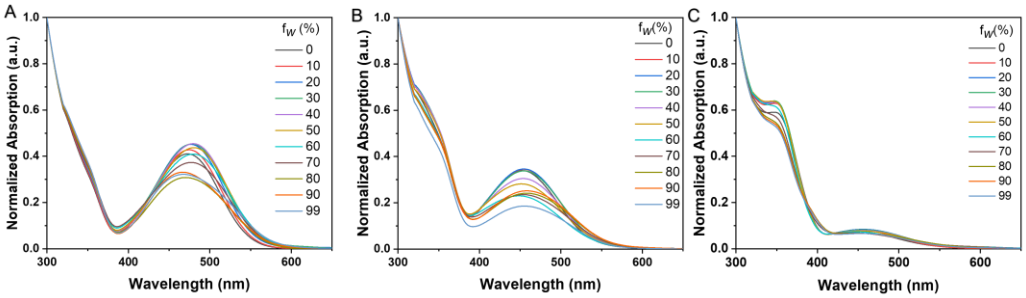

Figure S4. The normalized absorption spectra of **L1** (A), **L2** (B) and **L3** (C) in DMSO/H_2O mixture with different f_w (10 uM)

The quantum yield (QY) equation

$$QY\ (\%) = Q_R * \frac{I_s}{I_r}\frac{A_r}{A_s}\frac{{N_s}^2}{{N_r}^2} * 100$$

ΦR is the quantum yield of quinine bisulfate in 0.5 M sulfuric acid; A_y and Ar are the optical density (absorbance) of sample and Nile red, respectively; I_y and I_r are the integrated intensities (areas) of sample and standard spectra, respectively; the refractive indices of the sample and reference solution are N_y and N_r, respectively; The subscripts r and s stand for quinine sulfate and sample, respectively.

Compounds	QY (0%)	QY (90%)
L2	0.22% (0% H2O)	2.50% (90% H_2O)
L3	0.10% (0% H2O)	0.57% (90% H_2O)

Table S2. QY of **L2** and **L3** in solution (0% H_2O), aggregate state (99% H_2O) (Concentration= 10 μM)

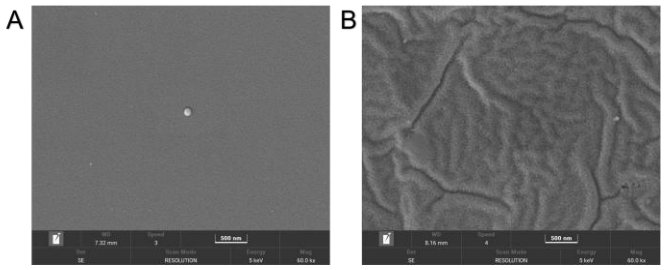

Figure S5. The SEM images of L2 (A) and (B) L3 in DMSO.

3. Crystallographic Data.

Identification code	**L1**
Empirical formula	$C_{26}H_{23}NO_4S$
Formula weight	445.51
Temperature/K	293.15
Crystal system	monoclinic
Space group	I_2/a
a/Å	17.7625(5)
b/Å	10.5502(2)
c/Å	25.8376(8)
α/°	90
β/°	107.111(3)
γ/°	90
Volume/Å^3	4627.6(2)
Z	8
ρcalcg/cm^3	1.279
μ/mm^{-1}	1.506
F(000)	1872.0
Crystal size/mm^3	0.3 × 0.04 × 0.04
Radiation	Cu Kα (λ = 1.54184)
2Θ range for data collection/°	7.16 to 179.114
Index ranges	-22 ≤ h ≤ 21, -10 ≤ k ≤ 13, -32 ≤ l ≤ 32
Reflections collected	21143
Independent reflections	4724 [R_{int} = 0.0584, R_{sigma} = 0.0331]
Data/restraints/parameters	4724/0/292
Goodness-of-fit on F^2	1.073
Final R indexes [I>=2σ (I)]	R_1 = 0.0420, wR_2 = 0.1139
Final R indexes [all data]	R_1 = 0.0577, wR_2 = 0.1265
Largest diff. peak/hole / e Å^{-3}	0.15/-0.26

Table S3. Crystal data and structure refinement for **L1**.

Atom	x	y	z	U(eq)
S01	4116.3(3)	6142.2(4)	2667.1(2)	62.44(15)
O003	3431.9(8)	8796.0(10)	5467.1(5)	62.3(3)
O006	3462.0(12)	10909.7(13)	5553.3(7)	92.0(5)
O007	3373.0(9)	6186.0(17)	2260.9(6)	91.4(5)
O00M	4482.9(12)	4941.0(14)	2817.1(7)	97.3(5)
N00D	3234.1(12)	3529.9(16)	6861.9(8)	80.2(5)
C009	3547.1(10)	7933.6(15)	5091.4(7)	53.9(4)
C00E	3407.2(10)	7741.8(16)	3207.3(7)	56.6(4)
C00G	3713.1(9)	8640.5(15)	4659.8(7)	52.6(4)
C00H	4016.6(9)	6889.5(14)	3255.5(7)	51.5(3)
C00I	3436.0(10)	4615.7(15)	5559.9(7)	57.4(4)
C00J	3711.4(10)	9896.9(15)	4773.6(7)	54.5(4)
C00L	3514.8(10)	6680.7(15)	5156.0(7)	54.5(4)
C00O	3284.9(12)	6421.0(16)	6070.4(7)	62.8(4)
C00P	3267.2(11)	4312.8(17)	6443.3(8)	61.2(4)
C00Q	4541.3(10)	6608.5(16)	3754.5(7)	57.1(4)
C00Y	3832.1(9)	8032.7(14)	4173.9(6)	51.1(3)
C00Z	4447.4(10)	7182.7(16)	4214.0(7)	57.2(4)
C012	3212.1(13)	5639.2(17)	6475.9(8)	68.3(5)
C015	3526.8(12)	10008.5(16)	5288.2(8)	64.1(4)
C016	3409.7(9)	5935.0(15)	5595.8(7)	52.6(4)
C017	3165.3(17)	2165(2)	6790.8(11)	93.9(7)
C01A	3366.8(11)	3824.6(15)	5962.9(8)	60.9(4)
C01B	3904.4(11)	10988.8(15)	4483.3(7)	56.5(4)
C01F	4470.9(12)	10879.6(19)	4211.6(8)	67.3(5)
C01H	4275.2(16)	13047(2)	3929.7(10)	87.9(7)
C01J	3720.3(15)	13175(2)	4203.5(10)	84.6(6)

C01L	3317.1(10)	8310.5(15)	3667.9(7)	55.0(4)
C01N	3536.2(13)	12155.7(17)	4479.8(9)	70.2(5)
C01O	4772.5(18)	7113(3)	2457.8(12)	107.8(9)
C01P	4656.3(14)	11902(2)	3940.4(9)	82.3(6)
C01S	3108(2)	4053(3)	7344.4(12)	122.0(12)

Table S4.Fractional Atomic Coordinates ($\times 10^4$) and Equivalent Isotropic Displacement Parameters ($Å2\times 10^3$) for **L1**-jiaben_auto. Ueq is defined as 1/3 of the trace of the orthogonalised UIJ tensor.

Identification code	**L2**
Empirical formula	C29H29NO5S
Formula weight	503.59
Temperature/K	293(2)
Crystal system	monoclinic
Space group	P21/c
a/Å	5.8445(2)
b/Å	26.0386(10)
c/Å	17.1880(6)
α/°	90
β/°	93.176(3)
γ/°	90
Volume/Å3	2611.70(16)
Z	4
ρcalcg/cm3	1.281
μ/mm 1	1.423
F(000)	1064.0
Crystal size/mm3	0.1 × 0.03 × 0.03
Radiation	Cu Kα (λ = 1.54184)
2Θ range for data collection/°	6.168 to 153.86
Index ranges	-5 ⩽ h ⩽ 7, -31 ⩽ k ⩽ 32, -21 ⩽ l ⩽ 21
Reflections collected	26496
Independent reflections	5341 [Rint = 0.0379, Rsigma = 0.0294]
Data/restraints/parameters	5341/12/330
Goodness-of-fit on F2	1.050

Final R indexes [I>=2σ (I)]	R1 = 0.0490, wR2 = 0.1357
Final R indexes [all data]	R1 = 0.0582, wR2 = 0.1422
Largest diff. peak/hole / e Å-3	0.45/-0.34

Table S5. Crystal data and structure refinement for **L2**.

Atom	x	y	z	U(eq)
S01	4671.8(8)	4663.2(2)	8580.1(3)	49.24(15)
O1	4095(3)	4167.7(6)	8269.4(10)	71.6(5)
O002	5039(2)	6585.5(5)	4784.9(8)	49.7(3)
O003	2437(3)	7215.3(6)	4804.2(10)	70.7(5)
O005	6812(3)	4718.3(8)	9010.0(11)	76.3(5)
N00J	-3445(4)	7447.7(9)	7901.4(15)	78.5(6)
C	2474(4)	4864.7(11)	9163.1(14)	70.1(6)
C00A	1137(3)	6784.6(7)	6380.1(11)	44.0(4)
C00B	8900(3)	5890.1(7)	4421.8(11)	46.0(4)
C00C	5720(3)	6182.5(7)	5265.9(10)	42.5(4)
C00D	3262(3)	6841.3(7)	5117.4(12)	48.7(4)
C00E	2706(3)	5449.4(8)	6649.4(11)	47.1(4)
C00F	2785(3)	5098.8(8)	7254.3(11)	48.8(4)
C00G	6330(3)	5792.1(8)	7105.6(12)	50.3(4)
C00H	7443(3)	5870.8(7)	5090.6(11)	45.1(4)
C00I	10852(3)	5582.9(8)	4430.4(12)	50.7(4)
C00K	1371(3)	6710.2(8)	7182.5(12)	50.5(4)
C00L	6387(3)	5453.7(8)	7728.1(12)	51.1(4)
C00M	-712(3)	7084.8(8)	6099.8(13)	53.5(5)
C00N	-1970(4)	7229.2(8)	7403.6(14)	58.5(5)
C00O	-2222(4)	7300.7(9)	6593.2(15)	61.1(5)
C00P	-125(4)	6924.9(9)	7683.3(13)	58.3(5)
C00Q	12318(4)	5596.0(9)	3823.5(14)	59.4(5)
C00R	8458(4)	6203.3(9)	3774.3(12)	58.9(5)
C00S	11874(4)	5913.3(9)	3197.4(14)	63.0(6)
C00T	9945(4)	6213.5(10)	3172.3(14)	67.0(6)
C00V	-5166(4)	7810.9(11)	7619(2)	87.8(9)
C00Y	-3080(7)	7364.9(13)	8734(2)	109.3(13)

C006	4472(3)	5799.1(7)	6566.4(10)	40.2(4)
C007	4616(3)	5108.7(7)	7796.5(10)	43.0(4)
C008	4294(3)	6183.9(7)	5931.6(10)	40.5(4)
C009	2803(3)	6582.2(7)	5855.4(10)	42.1(4)
O00W	10412(6)	3940.0(15)	10470(2)	146.3(11)
C00X	8992(7)	3700.9(14)	10069(3)	101.3(10)
C00Z	9530(9)	3505.1(16)	9295(3)	141.3(17)
C010	6718(9)	3609(2)	10319(3)	144.4(17)

Table S6. Fractional Atomic Coordinates ($\times 10^4$) and Equivalent Isotropic Displacement Parameters ($Å2\times 10^3$) for MN07_auto. Ueq is defined as 1/3 of the trace of the orthogonalised UIJ tensor.

Identification code	**L3**
Empirical formula	$C_{26}H_{23}NO_4S$
Formula weight	445.51
Temperature/K	100.00(10)
Crystal system	monoclinic
Space group	$P2_1/c$
a/Å	10.93180(10)
b/Å	27.3276(2)
c/Å	7.45150(10)
α/°	90
β/°	103.3310(10)
γ/°	90
Volume/Å^3	2166.08(4)
Z	4
ρcalcg/cm^3	1.366
μ/mm^{-1}	1.609
F(000)	936.0
Crystal size/mm^3	0.15 × 0.08 × 0.05
Radiation	Cu Kα (λ = 1.54184)
2Θ range for data collection/°	6.468 to 152.65
Index ranges	-13 ≤ h ≤ 13, -34 ≤ k ≤ 32, -6 ≤ l ≤ 9
Reflections collected	22411
Independent reflections	4423 [R_{int} = 0.0248, R_{sigma} = 0.0143]
Data/restraints/parameters	4423/0/292
Goodness-of-fit on F^2	1.034
Final R indexes [I>=2σ (I)]	R_1 = 0.0367, wR_2 = 0.0937
Final R indexes [all data]	R_1 = 0.0373, wR_2 = 0.0942
Largest diff. peak/hole / e Å^{-3}	0.29/-0.52

Table S7. Crystal data and structure refinement for **L3**.

Atom	x	y	z	U(eq)
S01	1027.3(3)	9350.1(2)	5713.8(4)	16.8(1)
O002	6075.7(9)	7864.3(3)	5652.5(13)	18.4(2)
O003	1079.7(9)	9480.8(4)	7600.2(14)	21.9(2)
O004	8105.6(9)	7970.3(4)	5548.0(14)	22.3(2)
O005	1477.5(10)	9701.1(4)	4573.7(15)	25.6(2)
N006	4300.3(12)	5117.2(5)	7153.6(19)	27.8(3)
C007	4144.9(13)	7524.6(5)	6042.3(18)	16.8(3)
C008	7257.2(13)	7154.8(5)	5860.4(18)	17.1(3)
C009	2969.7(12)	8819.1(5)	4997.1(18)	17.1(3)
C00A	3969.1(12)	5907.9(5)	5632.5(18)	17.3(3)
C00B	4723.3(13)	5577.5(5)	6863.1(19)	18.1(3)
C00C	5600.6(12)	6531.8(5)	6278.8(18)	16.2(3)
C00D	7280.4(12)	7691.5(5)	5684.5(18)	17.7(3)
C00E	5334.2(13)	7468.7(5)	5883.8(18)	16.7(3)
C00F	3725.5(12)	8407.1(5)	5096.7(18)	16.9(3)
C00G	5929.2(13)	5740.0(5)	7801.7(19)	19.4(3)
C00H	8363.4(13)	6856.1(5)	5771.8(18)	17.4(3)
C00I	6080.9(12)	7020.6(5)	5991.5(18)	16.3(3)
C00J	6346.0(12)	6204.7(5)	7516.5(19)	17.8(3)
C00K	2289.6(13)	7963.4(5)	6530.8(19)	17.8(3)
C00L	3401.6(12)	7973.0(5)	5884.9(18)	16.1(3)
C00M	1906.5(12)	8805.4(5)	5717.3(18)	16.5(3)
C00N	1550.4(13)	8377.4(5)	6480.1(19)	17.9(3)
C00O	4405.8(12)	6370.6(5)	5348.5(18)	16.9(3)
C00P	10458.0(13)	6293.3(5)	5559(2)	22.6(3)
C00Q	8219.2(13)	6423.5(5)	4732.3(19)	20.2(3)

C00R	9262.3(14)	6144.8(5)	4634(2)	22.6(3)
C00S	10606.8(13)	6723.5(5)	6580(2)	21.8(3)
C00T	9566.7(13)	7004.4(5)	6689(2)	20.2(3)
C00U	-528.3(13)	9185.7(5)	4654(2)	23.4(3)
C00V	5191.6(15)	4737.0(5)	7954(2)	25.8(3)
C00W	3038.8(14)	4961.0(5)	6244(2)	26.5(3)

Table S8. Fractional Atomic Coordinates (×10^4) and Equivalent Isotropic Displacement Parameters (Å2×10^3) for **L3**. Ueq is defined as 1/3 of the trace of the orthogonalised UIJ tensor.

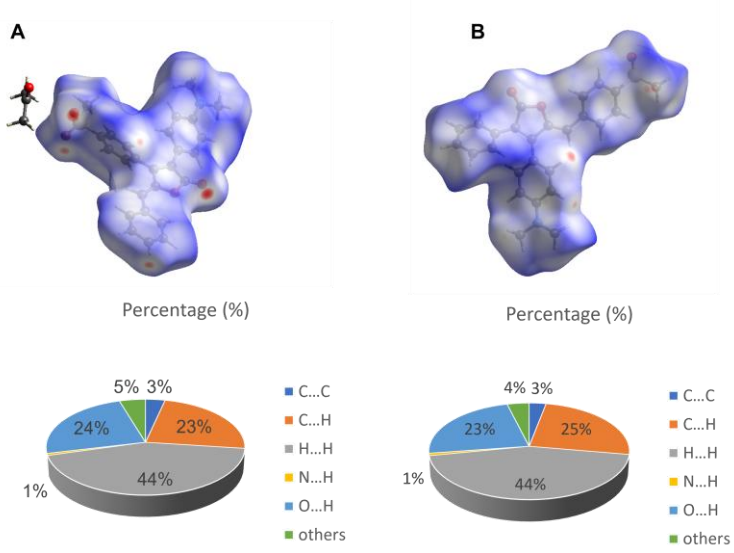

Figure S6 Hirshfeld surfaces mapped with d norm for **L2** and **L3** and the weak interaction forces present in the **L2** and **L3** crystal and their percentages.

4. Trace water

	mg/mL	Karl Fischer reagent(mL)
1	3.6647	2.6002
2	3.802	2.6976
3	3.8542	2.7337
4	3.8921	2.7615

Table S9： Data for Karl Fischer Reagent Standard Titration.

M1(g) a	M2(g) b	ΔM(g)c	Karl Fischer reagent(mL) d	fw(%)e	Average fw(%)
2.1144	1.8222	0.2922	0.9383	1.19	1.175
2.1547	1.86066	0.29404	0.9204	1.16	

Table S10. Calculation of water content by the Karl Fischer method. a: Weight of the bottle before titration; b: Weight of the bottle after titration; c: Sample weight; d: Volume of Karl Fischer reagent; e: Water content.

5. Acidochromism

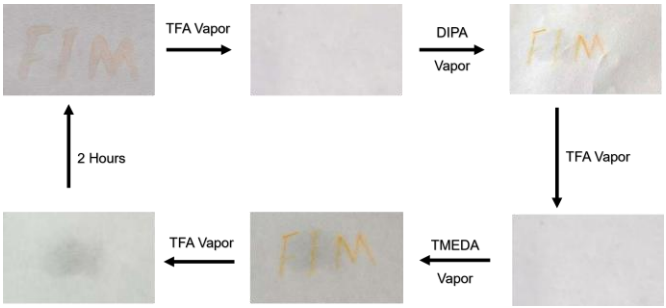

Figure S7. "FIM" written with MeOH solution of **L2** on a piece of filter paper then fumigated with TFA and DIPA and TMEDA in turn (10 mM).

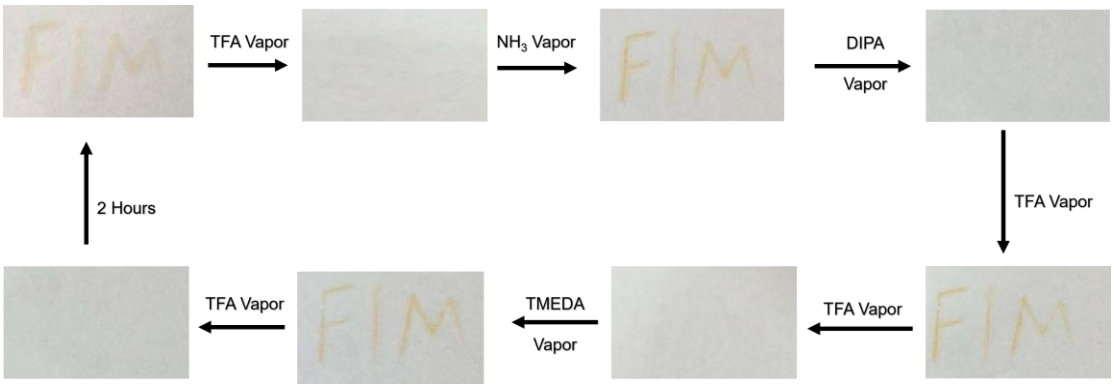

Figure S8 "FIM" written with MeOH solution of **L3** on a piece of filter paper then fumigated with TFA and NH_3, DIPA and TMEDA in turn (10 mM).

6. Confocal image

Cell Viability after Photoactivation Treatment

MCF-7 cells were cultured at a density of 5×10^3 cells per well in a 96-well plate for 72 hours. Then the cells were treated with the medium containing diverse concentration of **L2** and **L3** for 30 minutes, and then exposed to either darkness or 365 nm laser irradiation (48 mW/cm²) for 20 minutes. After being incubated for 72 hours, 10 μL of Cell Counting Kit - 8 (CCK8, DOJINDO, Japan) was added to the cells, and the incubation was continued for 1 hour at 37°C. The cell viability was determined by measuring the absorbance at 490 nm using a multifunctional microplate reader (TECAN, M200 PRO, Switzerland), and the results were expressed as the relative ratio of cell viability in comparison with the untreated control.

Cell Culture and Imaging in MCF-7 Cells

MCF-7 cells were cultivated on a confocal dish for 24 hours. Then, the culture medium was substituted with a medium that contained 10 μM **L2** and **L3** as well as BODIPY 503. After incubation for 30 min, these cells were washed with PBS and resuspended in fresh medium. After two minutes of light irradiation at 405nm (48 mW/cm²), images were immediately acquired using a confocal microscope (Leica, STELLARIS 5, Germany), employing consistent acquisition parameters across all experimental groups. Green Channel of BODIPY 503 was at 500-550 nm with excitation at 488 nm. Red Channel of **L2** and **L3** were at 575-840 nm with excitation at 405 nm.

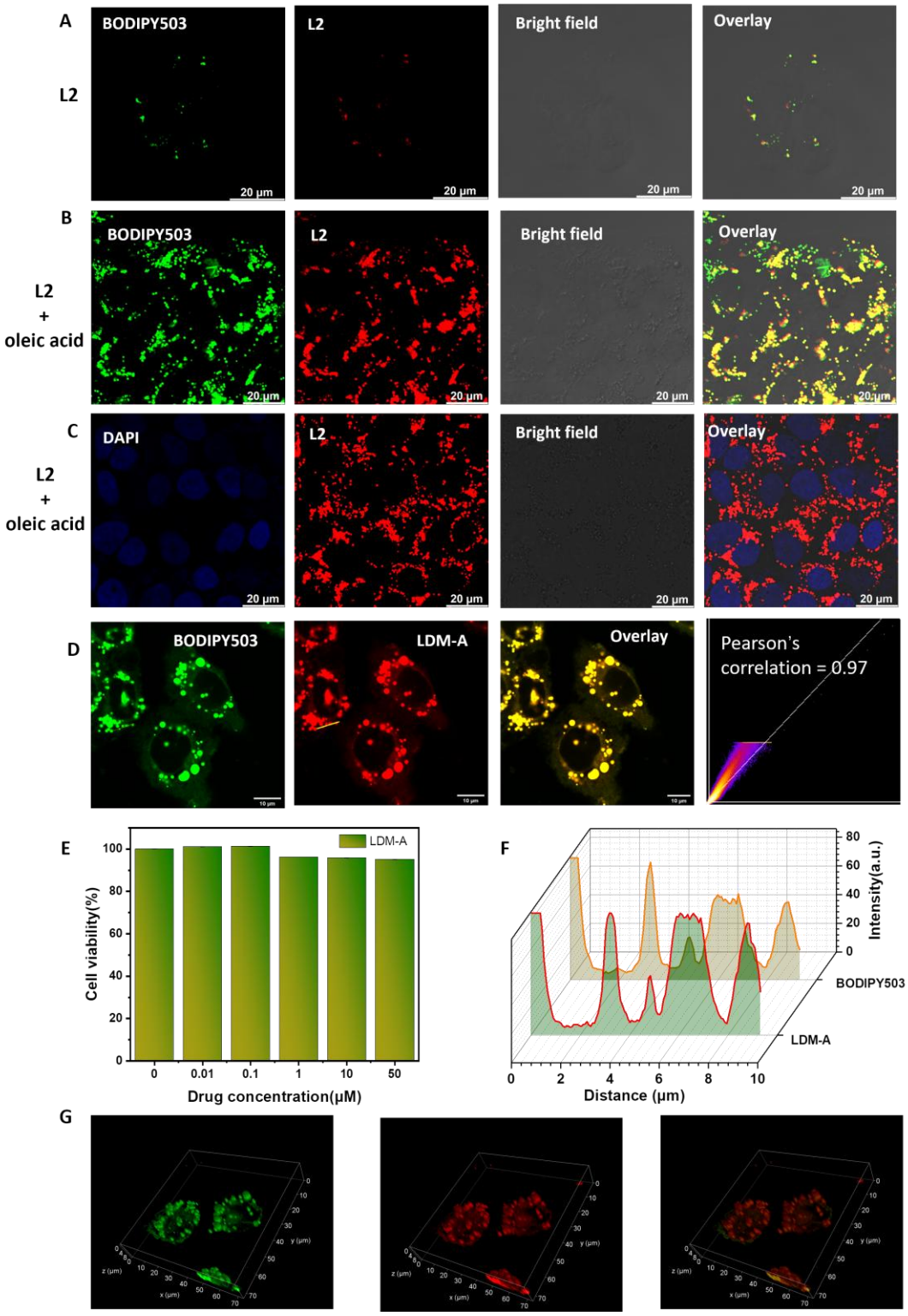

Figure S9 A. B. Fluorescence microscopy images of MCF-7 cell stained with **L2** and BODIPY503 (scale bar: 20 μm) C. Fluorescence microscopy images of MCF-7 cell stained with L2 and DAPI (scale bar: 20 μm). D. Fluorescence microscopy images of MCF-7 cell stained with **L3** and BODIPY503 (scale bar: 20 μm, Green channel: λ_{ex} = 405 nm, λ_{em} = 420 − 550 nm; red channel: λ_{ex} = 633 nm, λ_{em} = 650 − 850 nm), which have been supplemented with oleic

acid (0.1 mM, 24 h) before fixation. E. Cell viability of **L2** after 24h with MCF-7 cells. F The 2D intensity histogram for L2. G. 3D confocal image of fixed MCF-7 cells labelled with **L3** and the BODIPY503

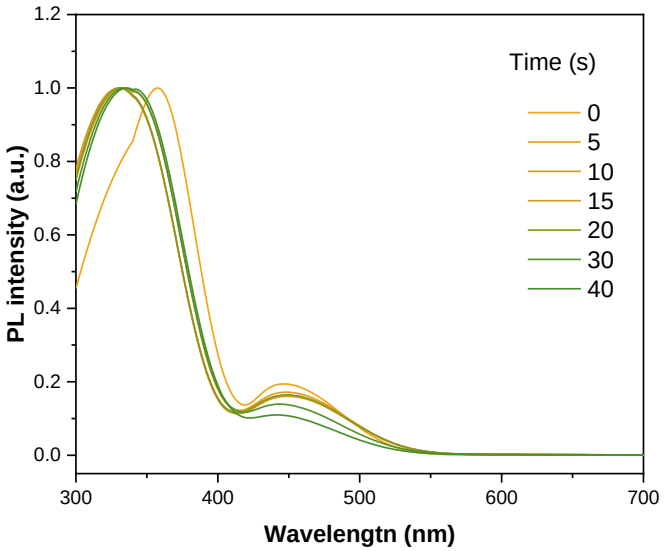

Figure S10 Change in the absorption spectrum with the photoisomerization of **L3** to **L3-E** under 365 LED irradiation (46 mW/cm^2)

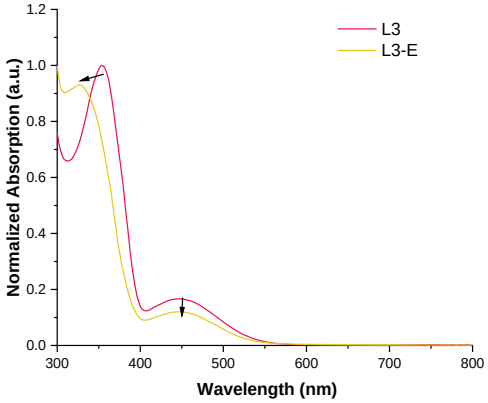

Figure S11 Comparison of absorption spectra between **L3** and **L3-E.**

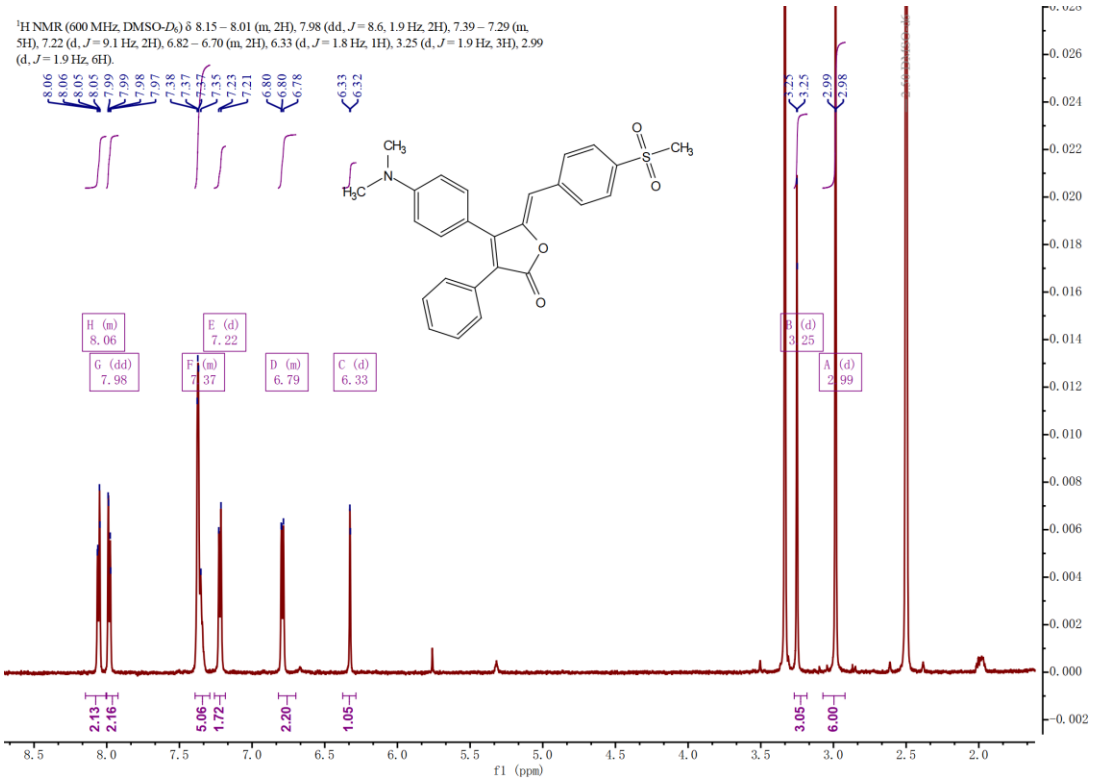

Figure S12 ^{1}H NMR Spectra of **L3** (600 MHz, DMSO-d_6).

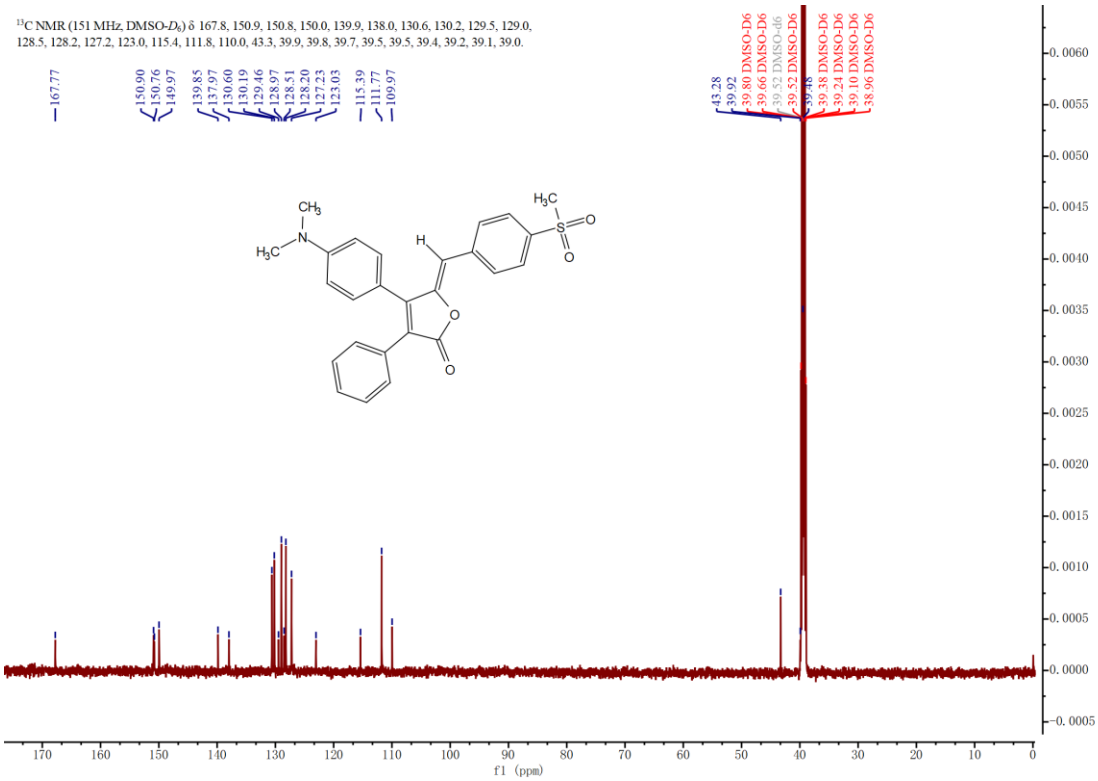

Figure S13 ^{13}C NMR Spectra of **L3** (600 MHz, DMSO-d_6).

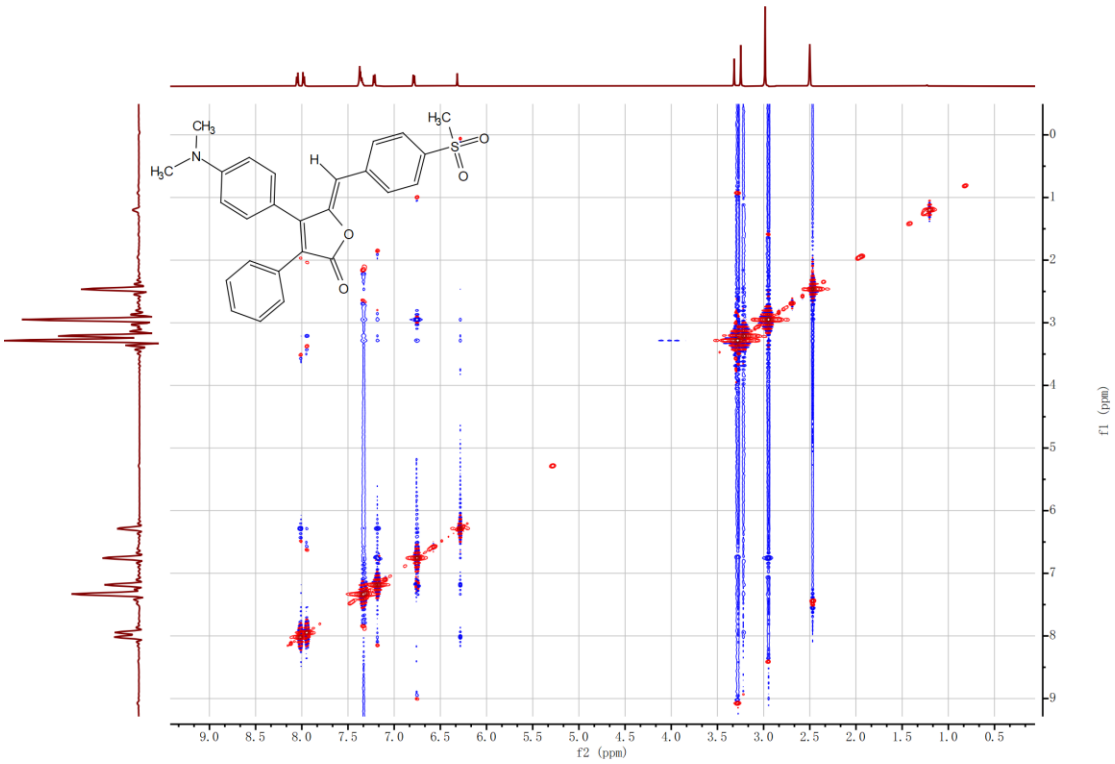

Figure S14. ROESY spectrum of L3 in DMSO-d_6.

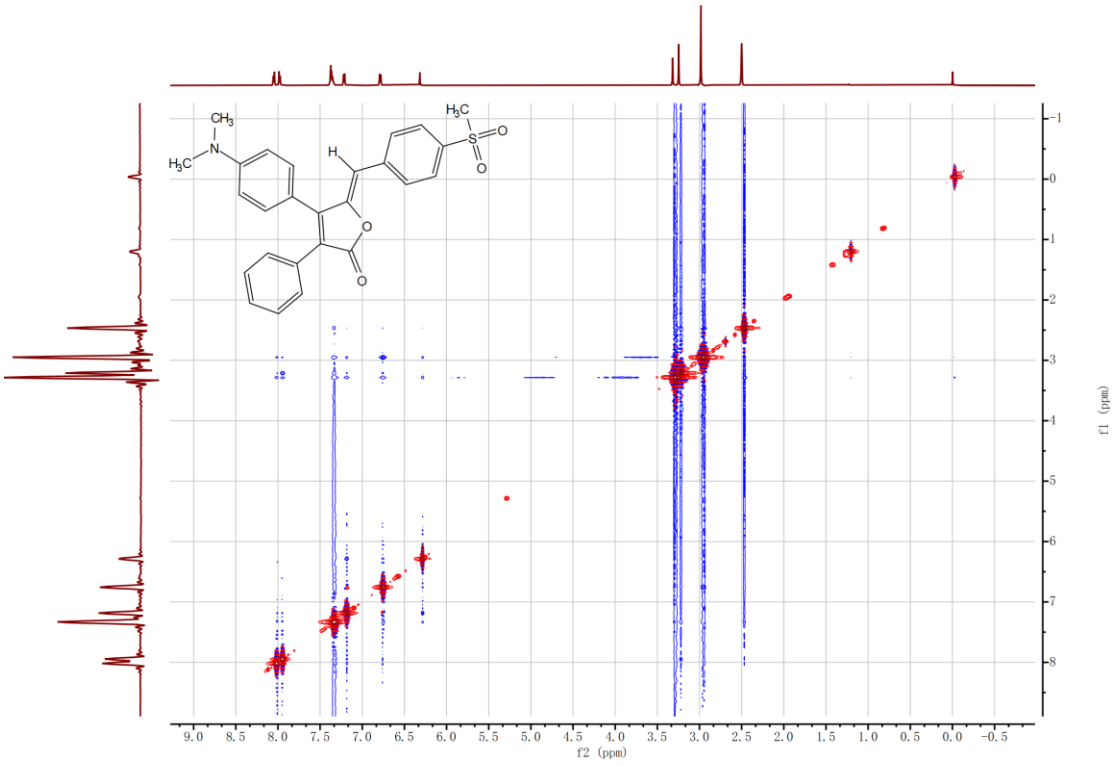

Figure S15. NOESY spectrum of L3 in DMSO-d_6.

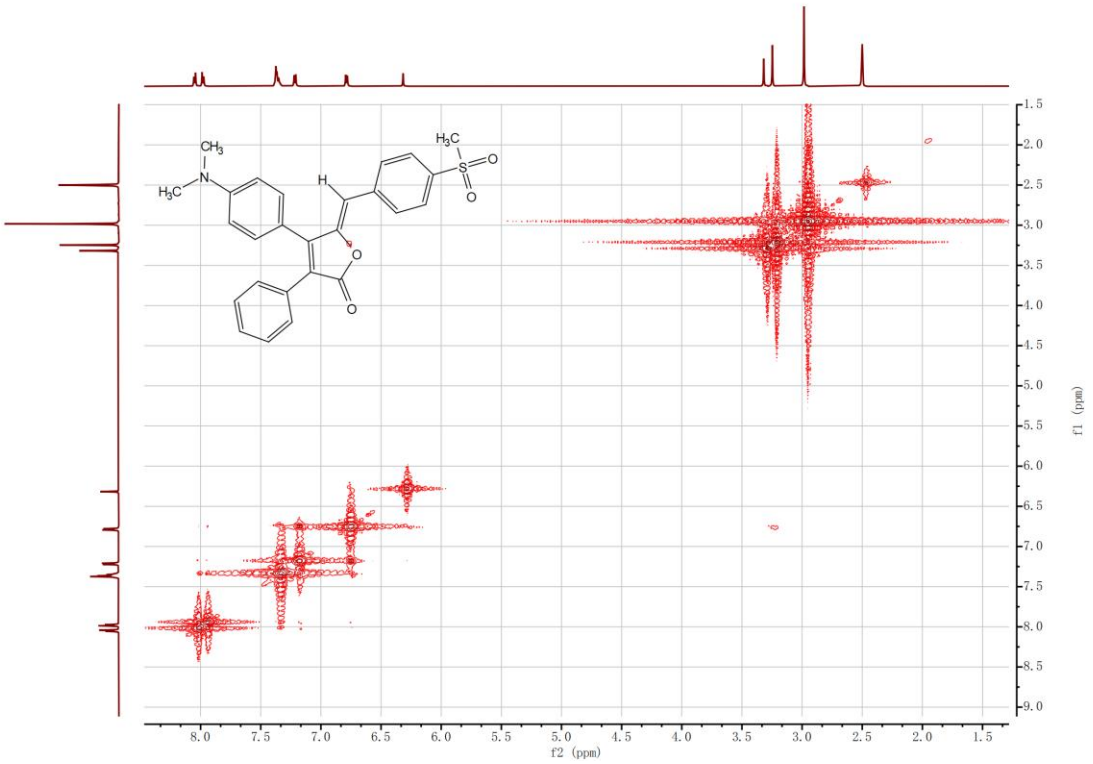

Figure S16. ^{1}H-^{1}H COSY spectrum of L3 in DMSO-d_6.

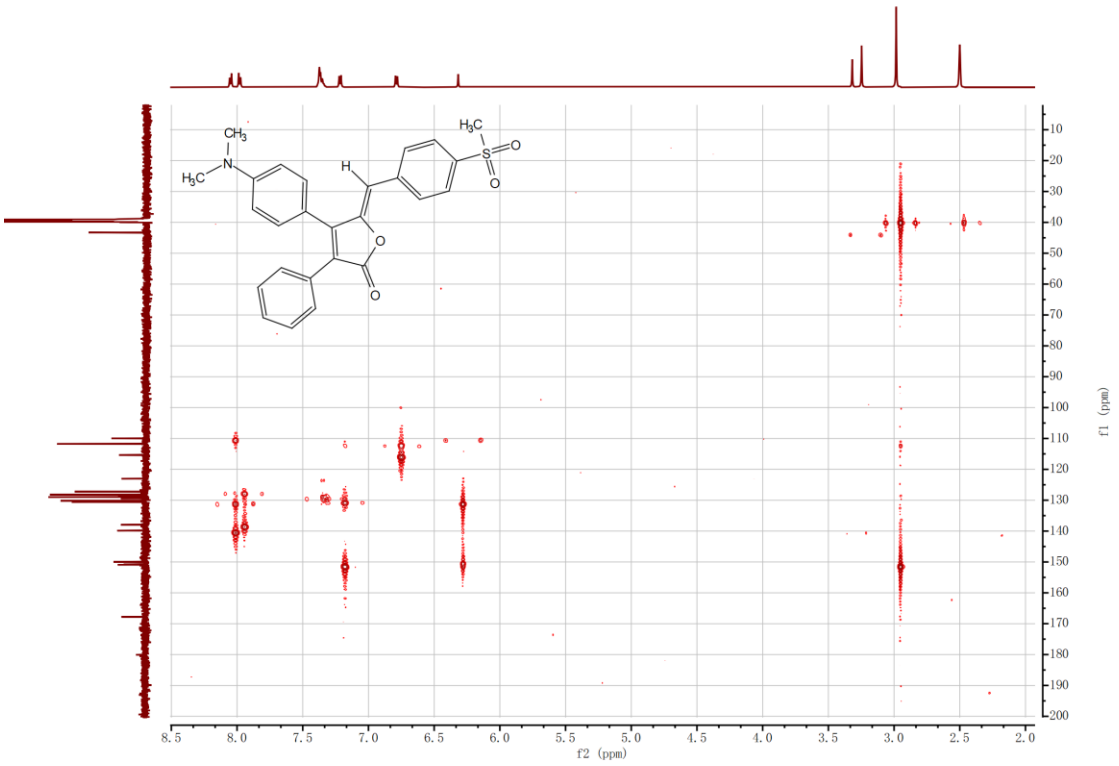

Figure S17. HMBC spectrum of L3 in DMSO-d_6.

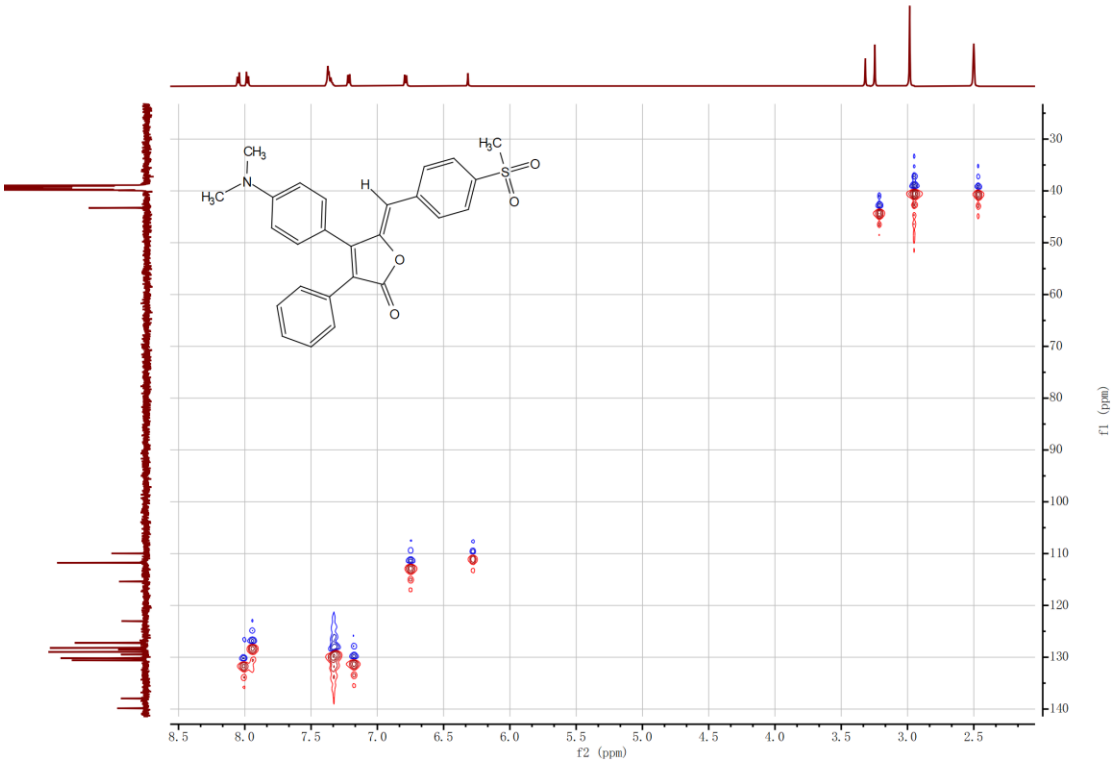

Figure S18. HSQC spectrum of L3 in DMSO-d_6.

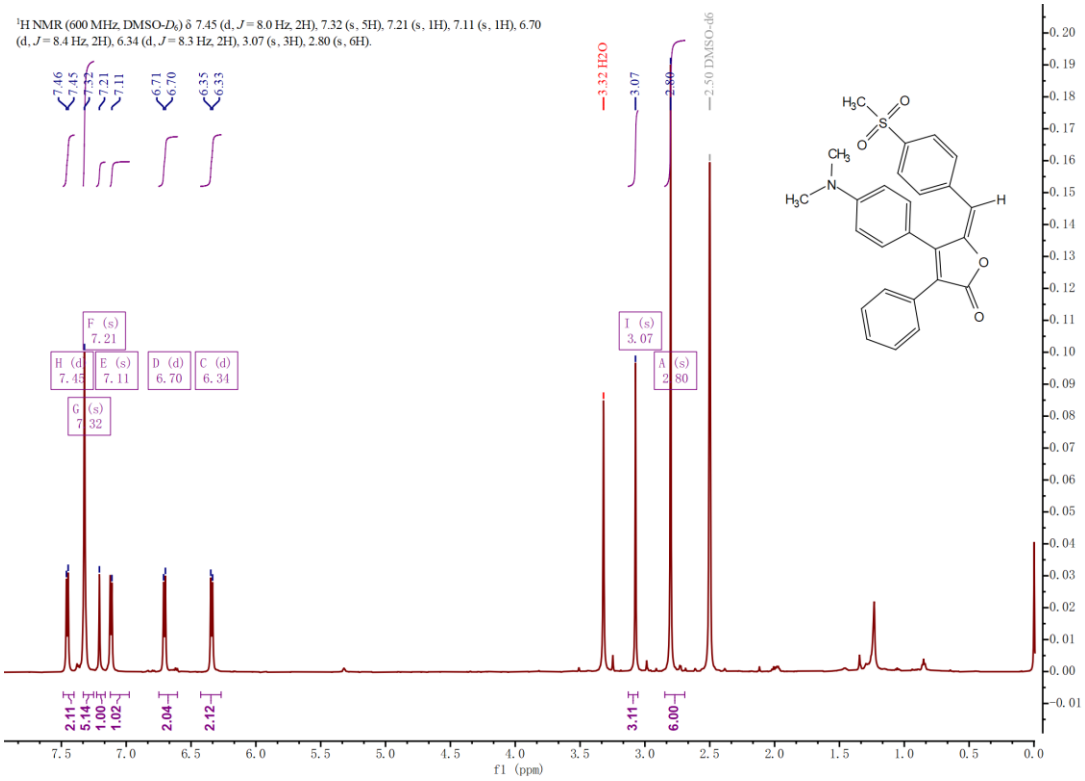

Figure S19. ¹H NMR Spectra of **L3-E** (600 MHz, DMSO-d_6).

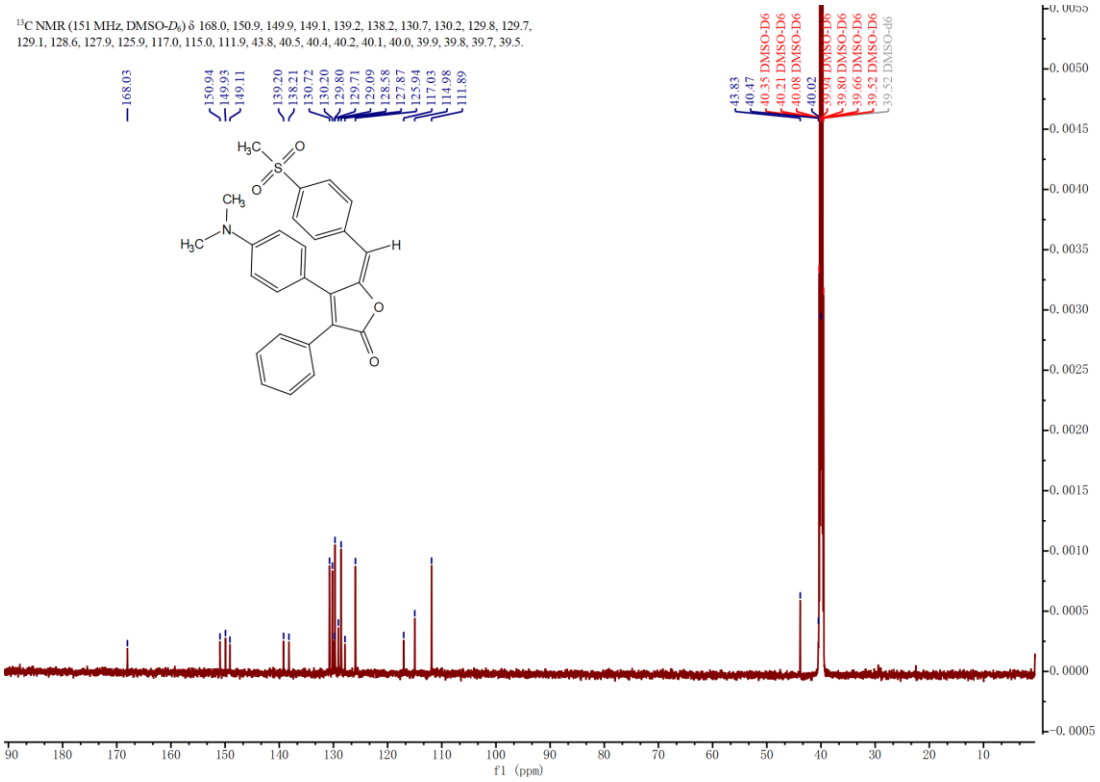

Figure S20. ^{13}C NMR Spectra of **L3-E** (600 MHz, DMSO-d_6).

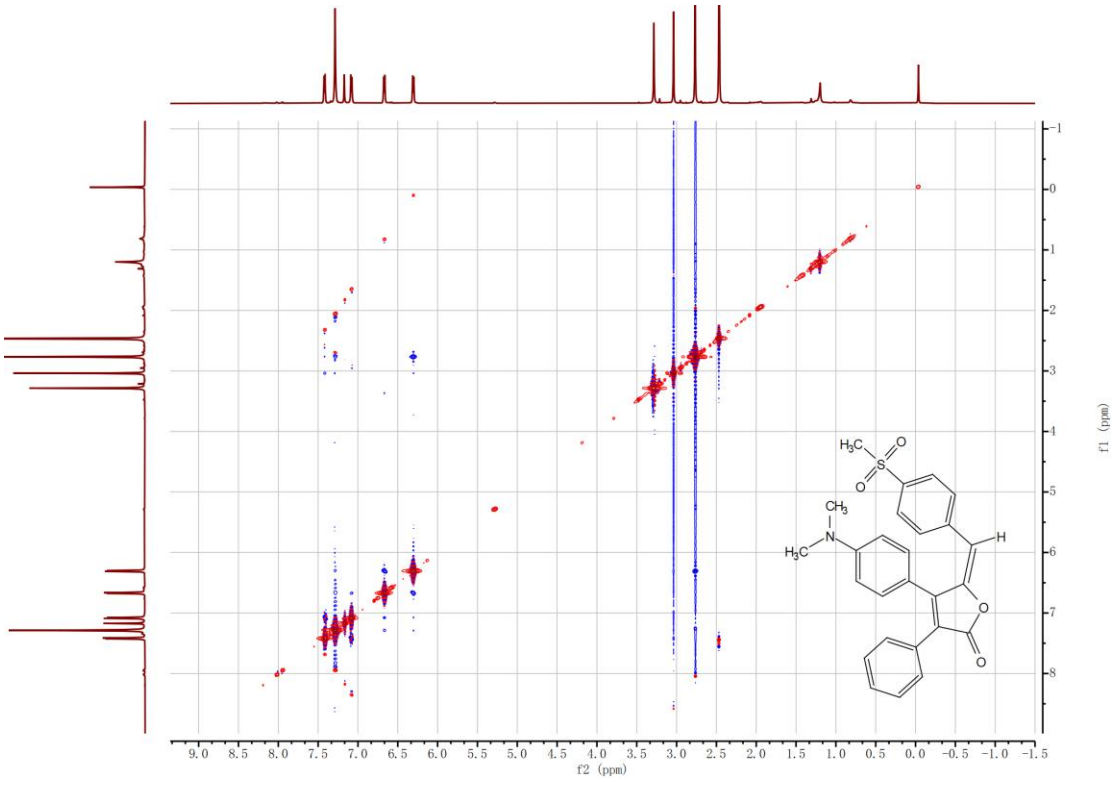

Figure S21. ROESY spectrum of L3-E in DMSO-d_6.

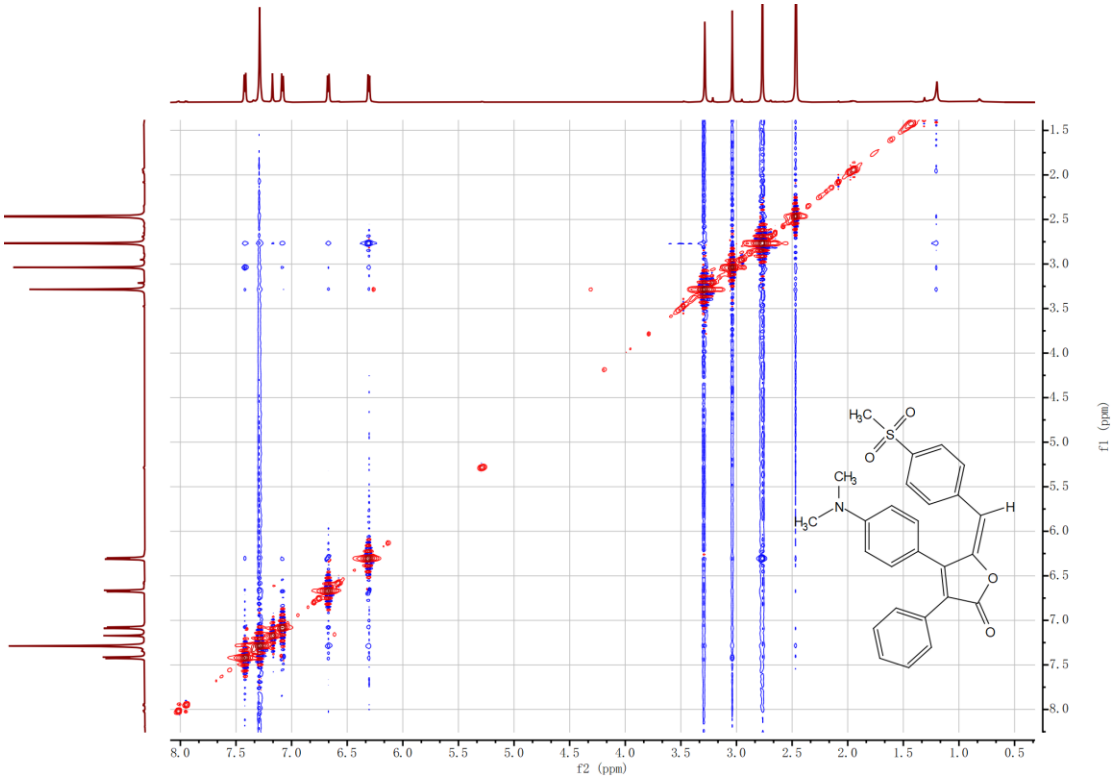

Figure S22. NOESY spectrum of L3-E in DMSO-d_6.

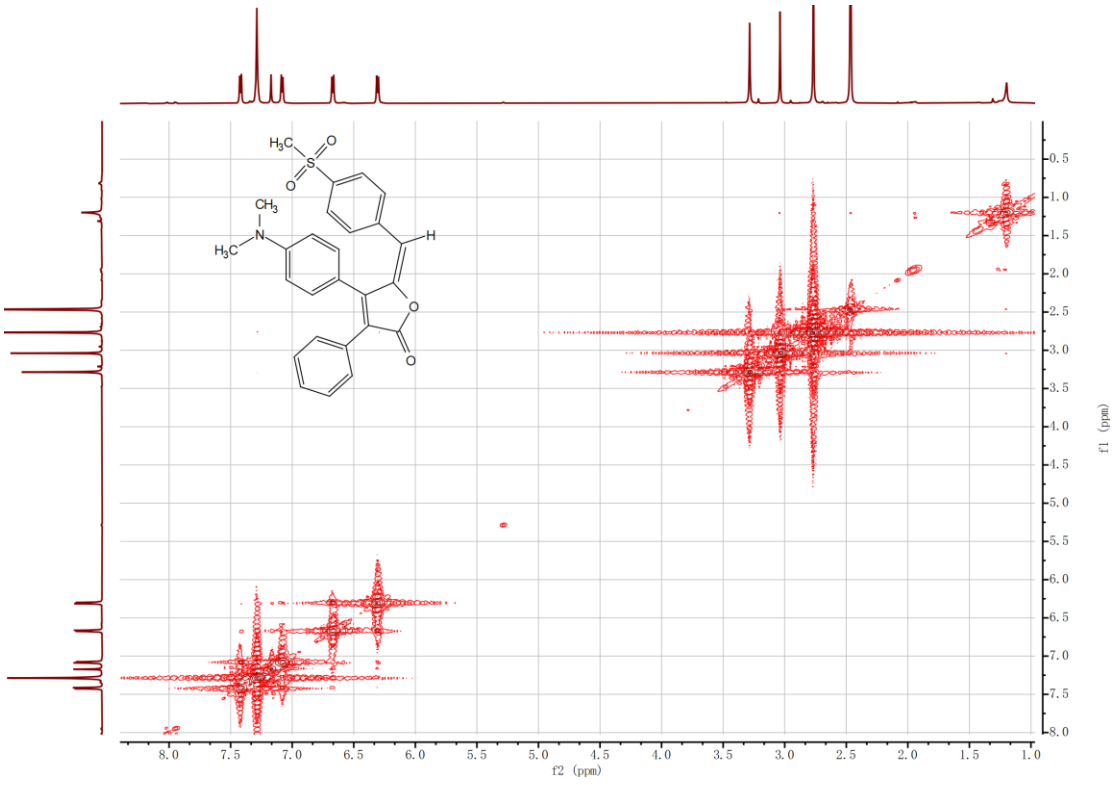

Figure S23. ^{1}H-^{1}H COSY spectrum of L3-E in DMSO-d_6.

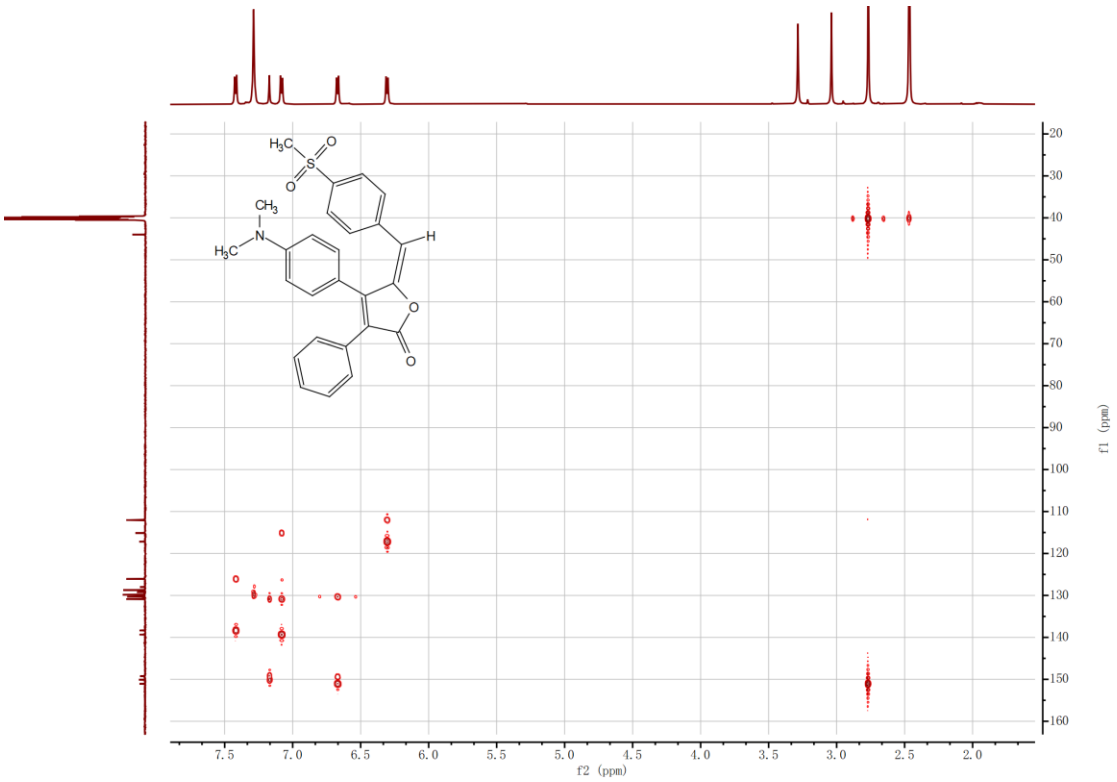

Figure S24. HMBC spectrum of L3-E in DMSO-d_6.

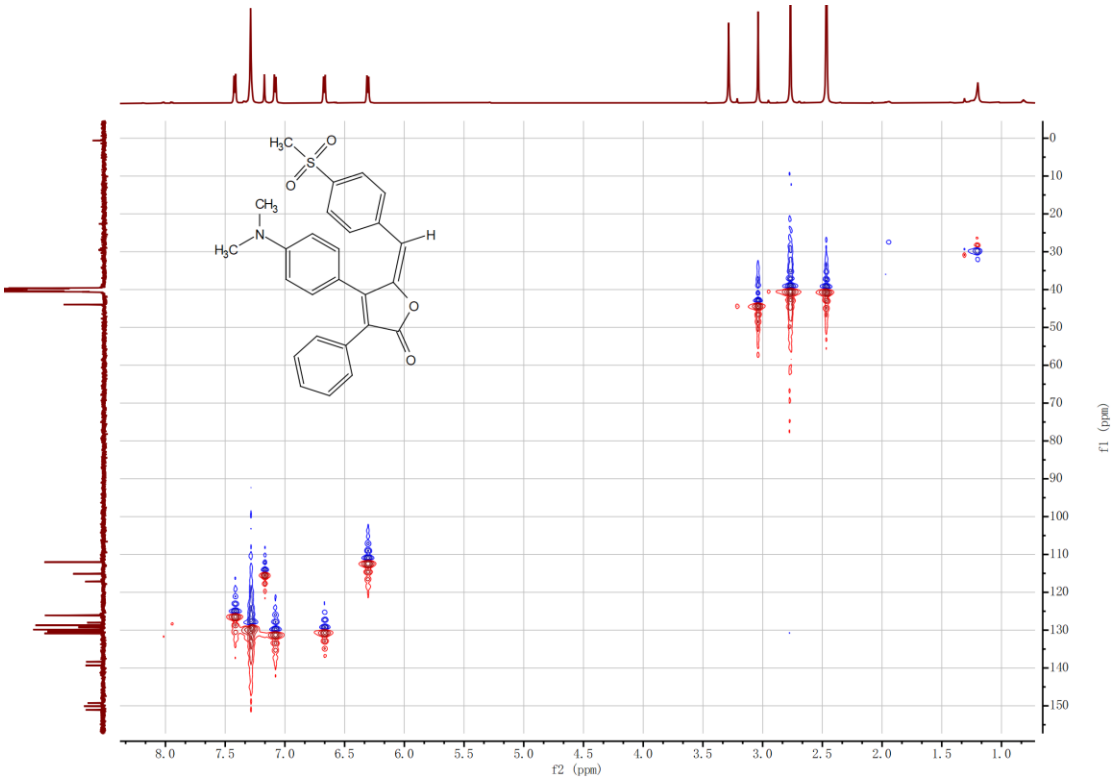

Figure S25. HSQC spectrum of L3 in DMSO-d_6.

7. Characterization of L1, L2 and L3

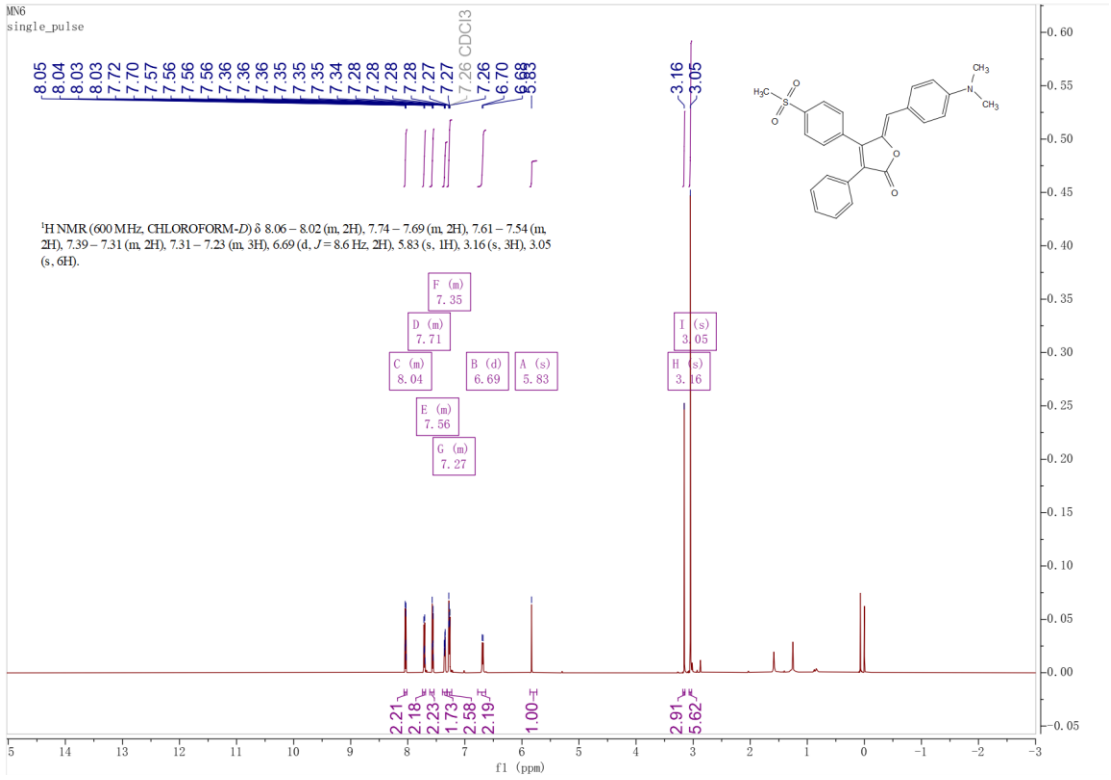

Figure S26. ^{1}H NMR Spectra of **L1** (600 MHz, C*D*Cl$_3$).

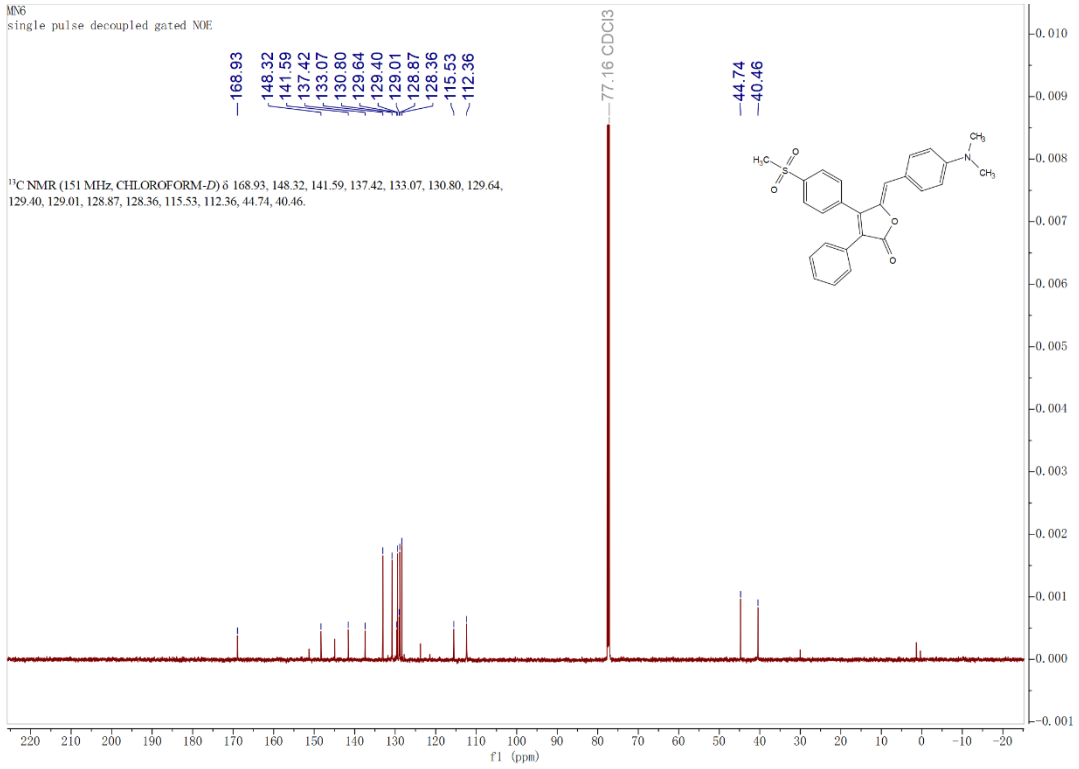

Figure S27. ^{13}C NMR Spectra of **L1** (600 MHz, C*D*Cl$_3$).

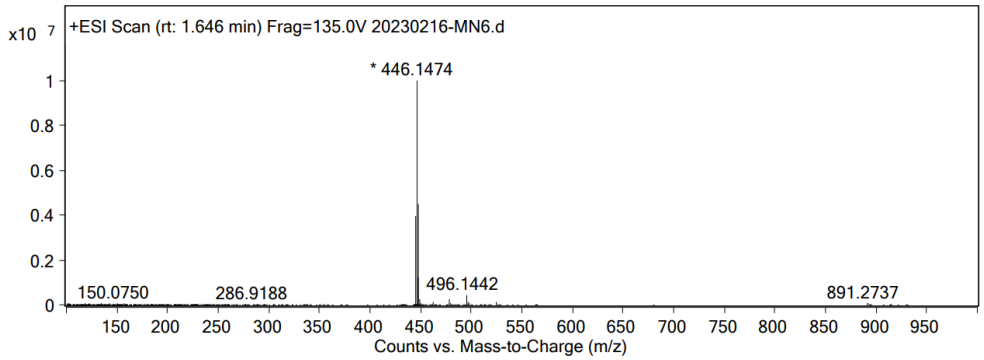

Figure S28. HRMS spectrum of **L1**.

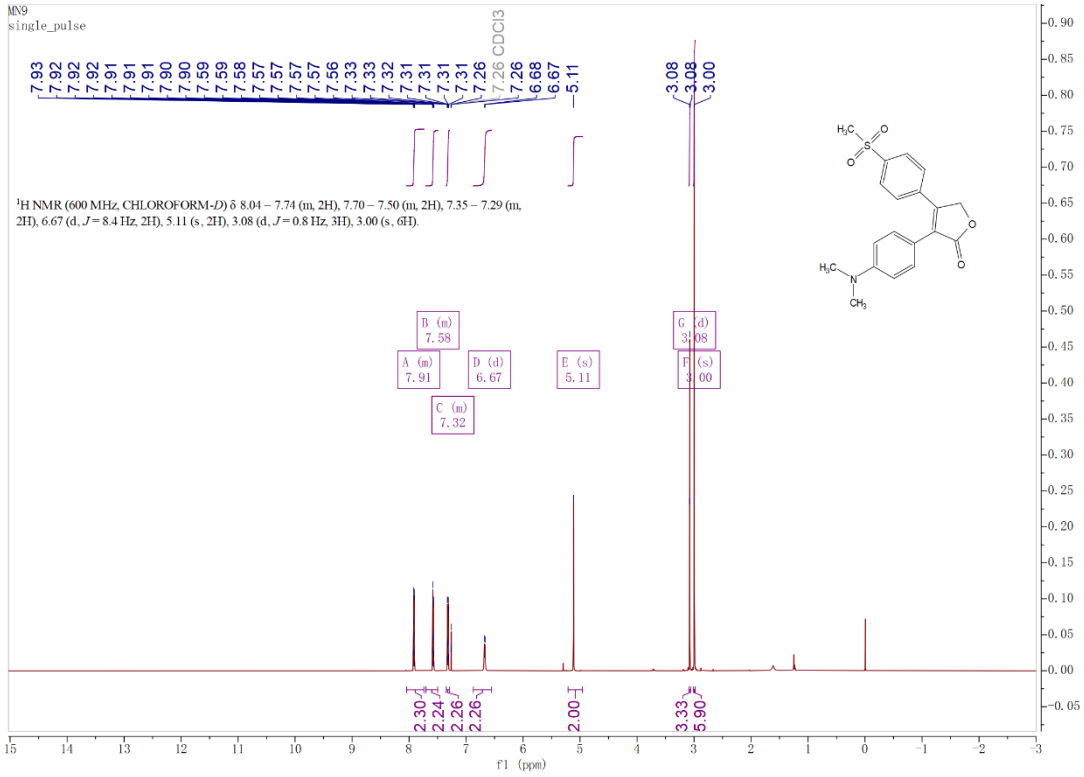

Figure S29. ^{1}H NMR Spectra of **L2-0** (600 MHz, *C*DCl_3)**.**

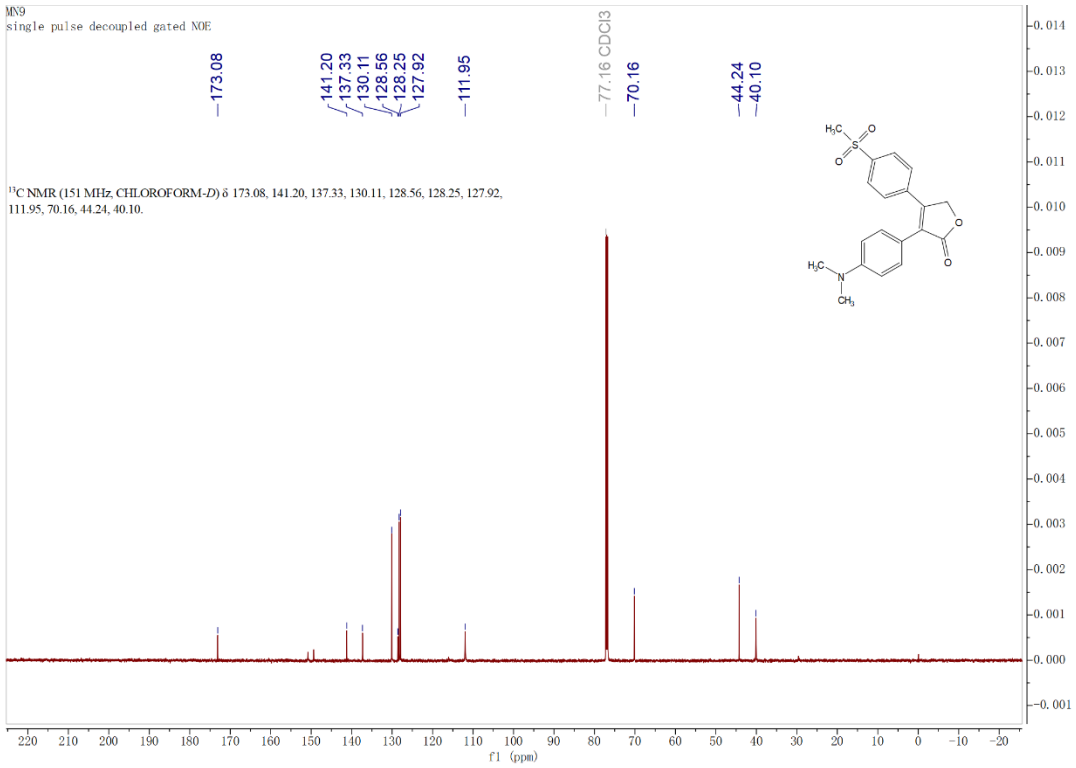

Figure S30. ^{13}C NMR Spectra of **L2-0** (600 MHz, $CDCl_3$).

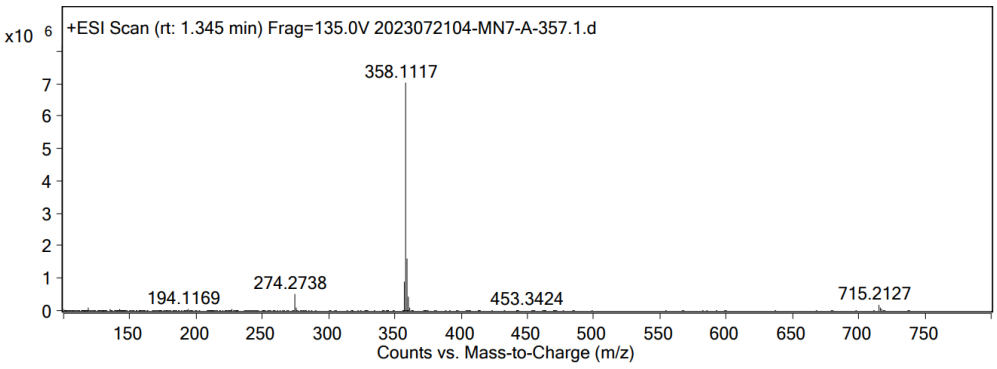

Figure S31. HRMS spectrum of **L2-0**

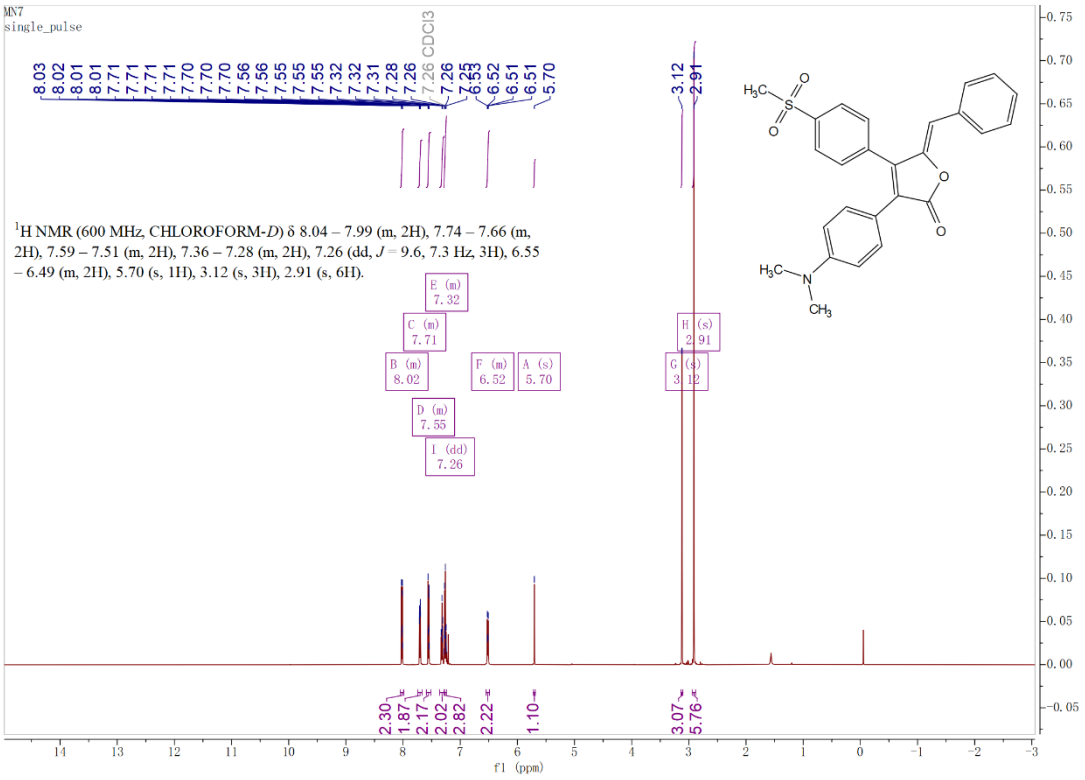

Figure S32. ^{1}H NMR Spectra of **L2** (600 MHz, C*D*Cl$_3$).

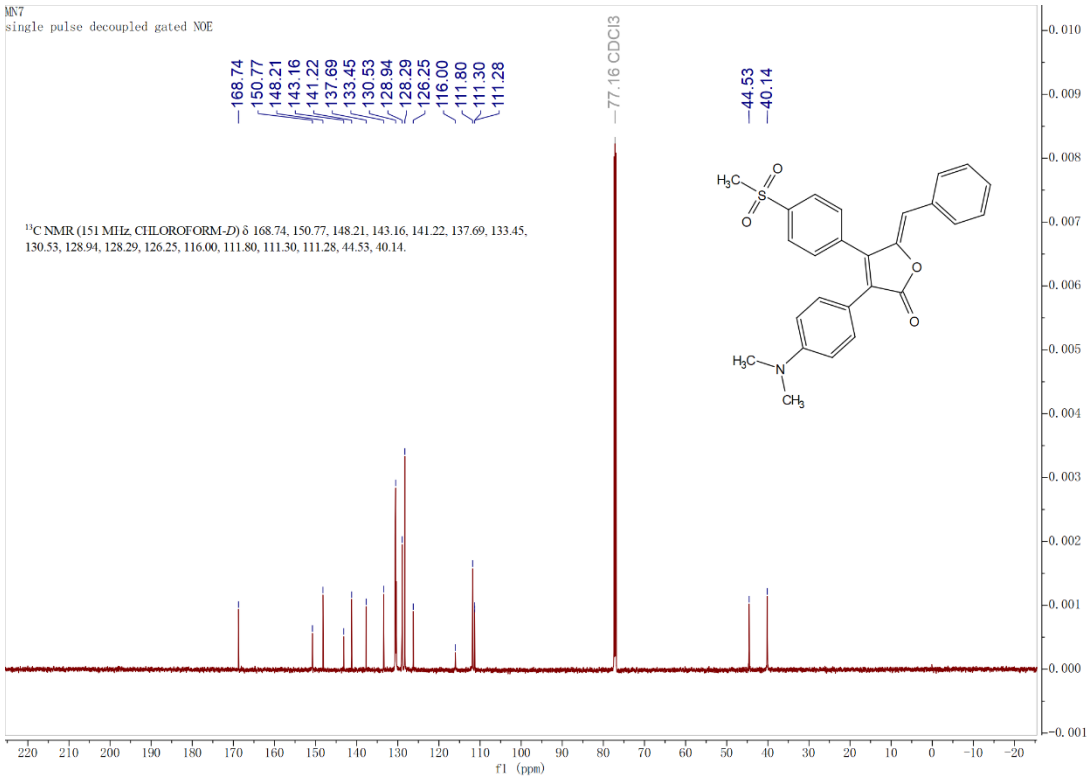

Figure S33. ^{13}C NMR Spectra of **L2** (600 MHz, C*D*Cl$_3$).

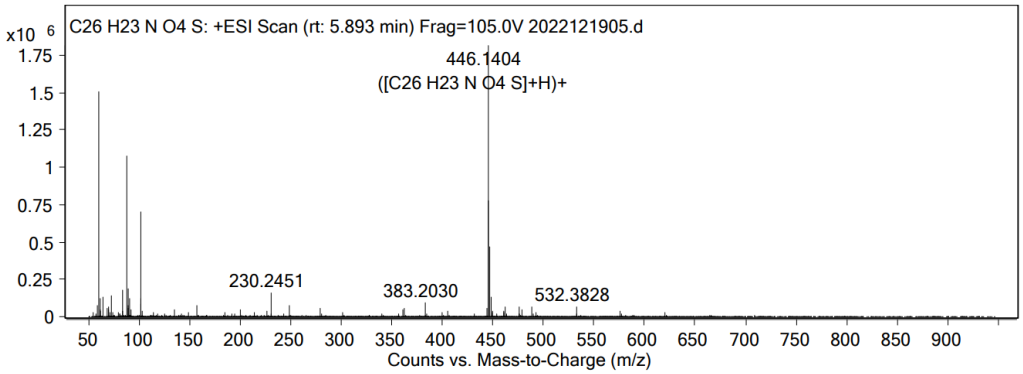

Figure S34. HRMS spectrum of **L2**.

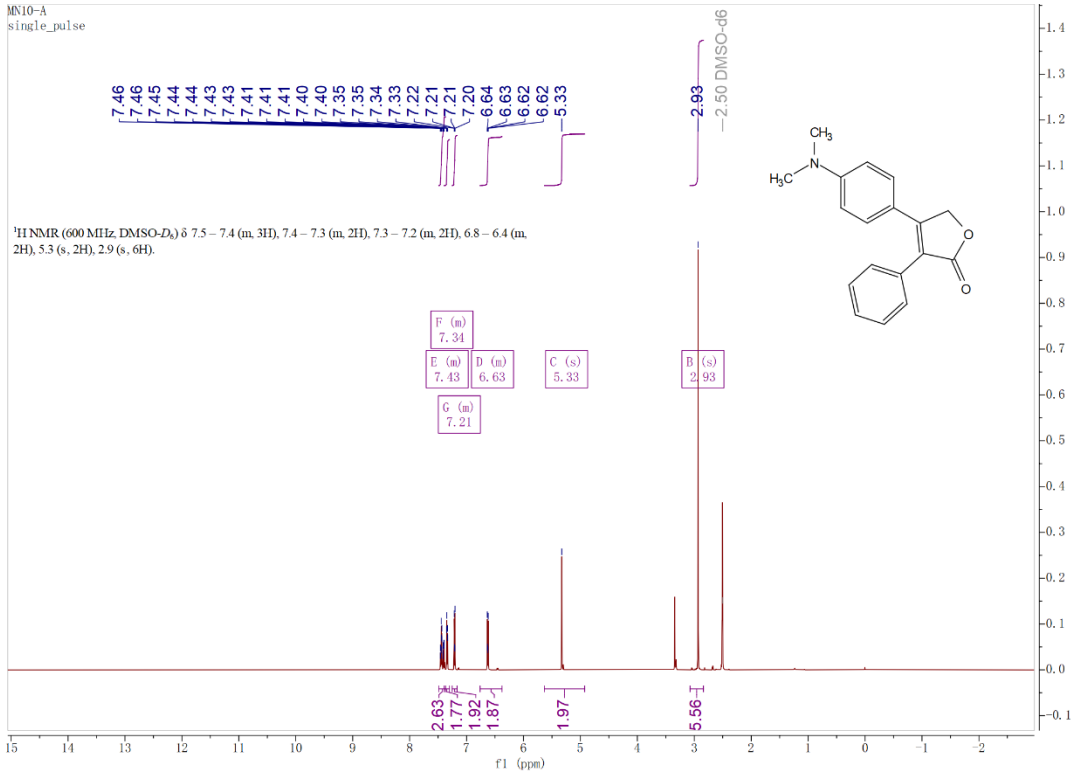

Figure S35. ^{1}H NMR Spectra of **L3-0** (600 MHz, DMSO-d_6)**.**

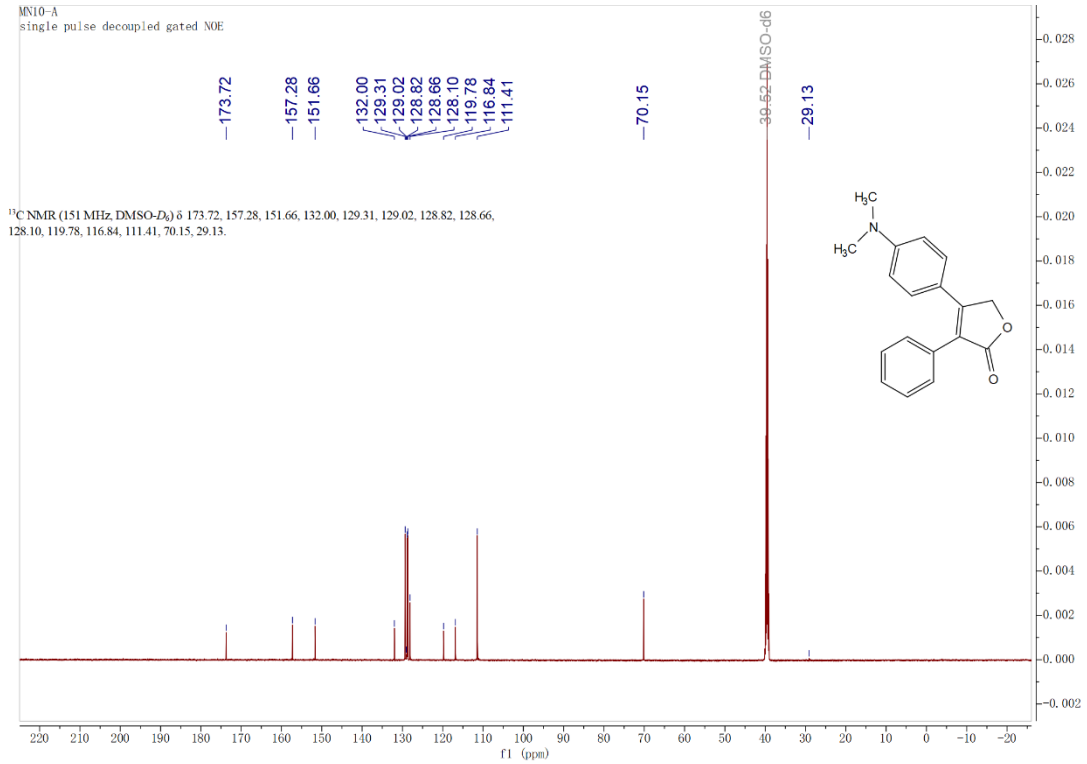

Figure S36. ^{13}C NMR Spectra of **L3-0** (600 MHz, DMSO-d_6).

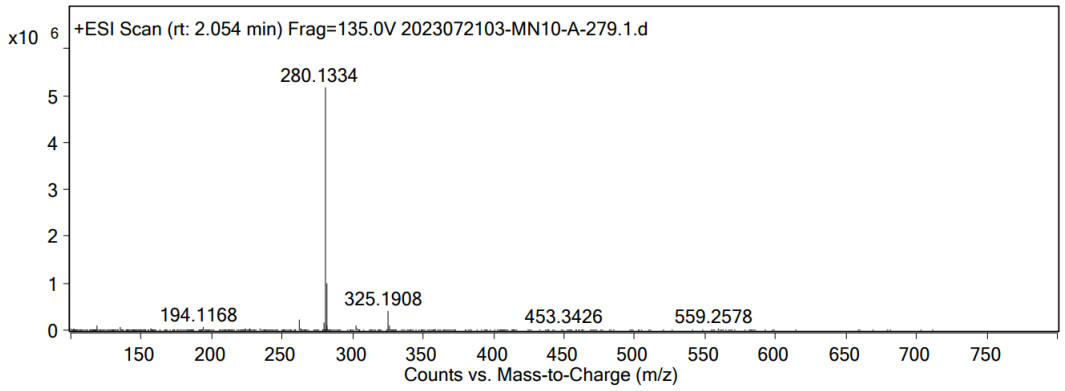

Figure S37. HRMS spectrum of **L3-0**

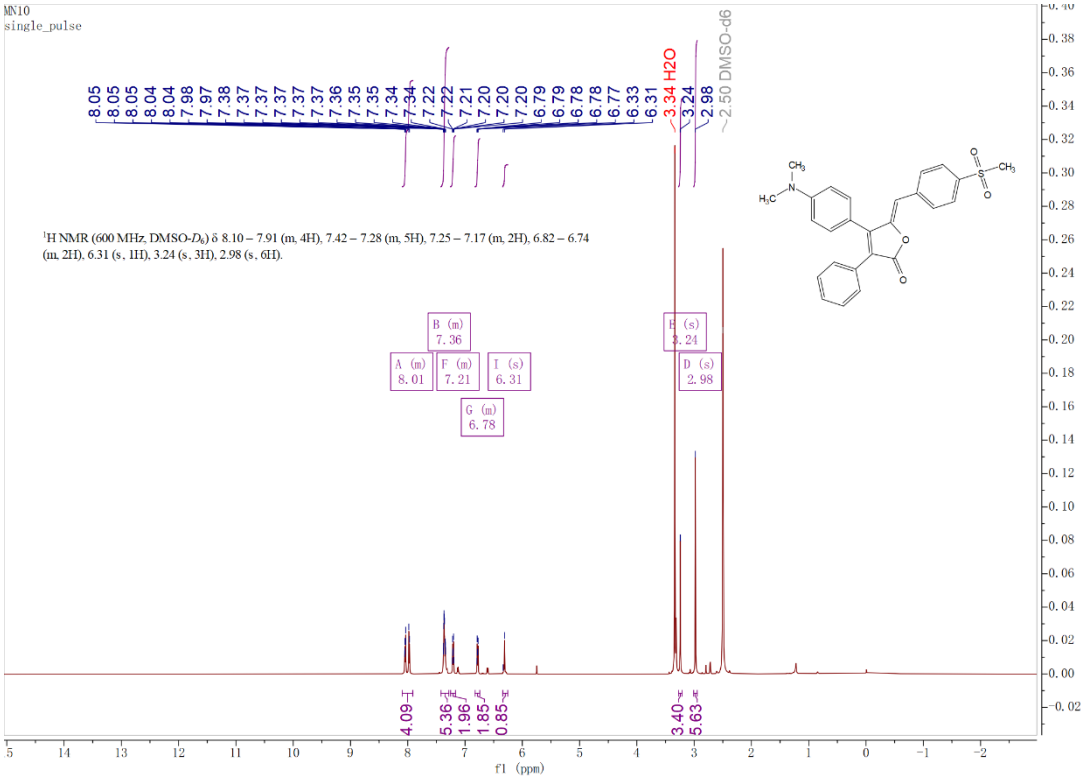

Figure S38. ^{1}H NMR Spectra of **L3** (600 MHz, DMSO-d_6).

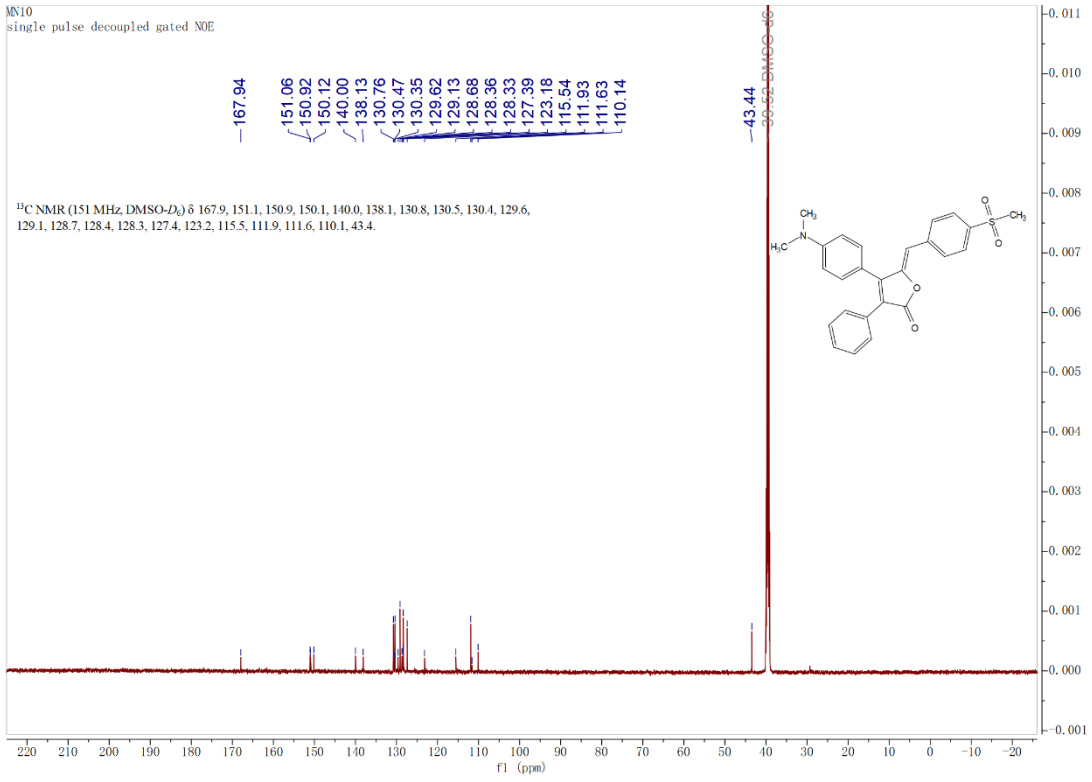

Figure S39 ^{13}C NMR Spectra of **L3** (600 MHz, DMSO-d_6).

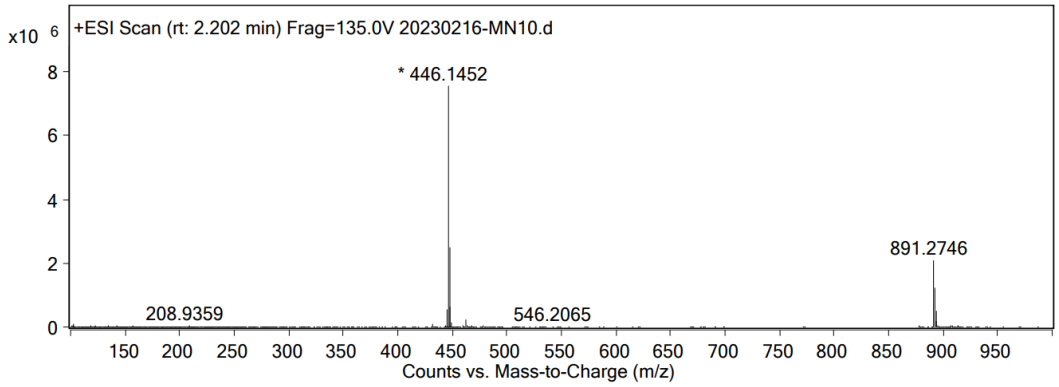

Figure S40. HRMS spectrum of **L3**.